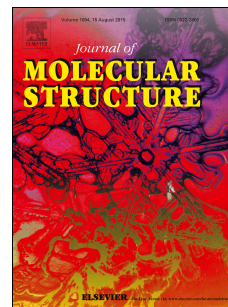


Accepted Manuscript

Effect of azo and ester linkages on rod shaped Schiff base liquid crystals and their photophysical investigations

Chinnaiyan Selvarasu, Palaninathan Kannan



PII: S0022-2860(16)30668-8

DOI: [10.1016/j.molstruc.2016.06.081](https://doi.org/10.1016/j.molstruc.2016.06.081)

Reference: MOLSTR 22700

To appear in: *Journal of Molecular Structure*

Received Date: 13 April 2016

Revised Date: 28 June 2016

Accepted Date: 28 June 2016

Please cite this article as: C. Selvarasu, P. Kannan, Effect of azo and ester linkages on rod shaped Schiff base liquid crystals and their photophysical investigations, *Journal of Molecular Structure* (2016), doi: 10.1016/j.molstruc.2016.06.081.

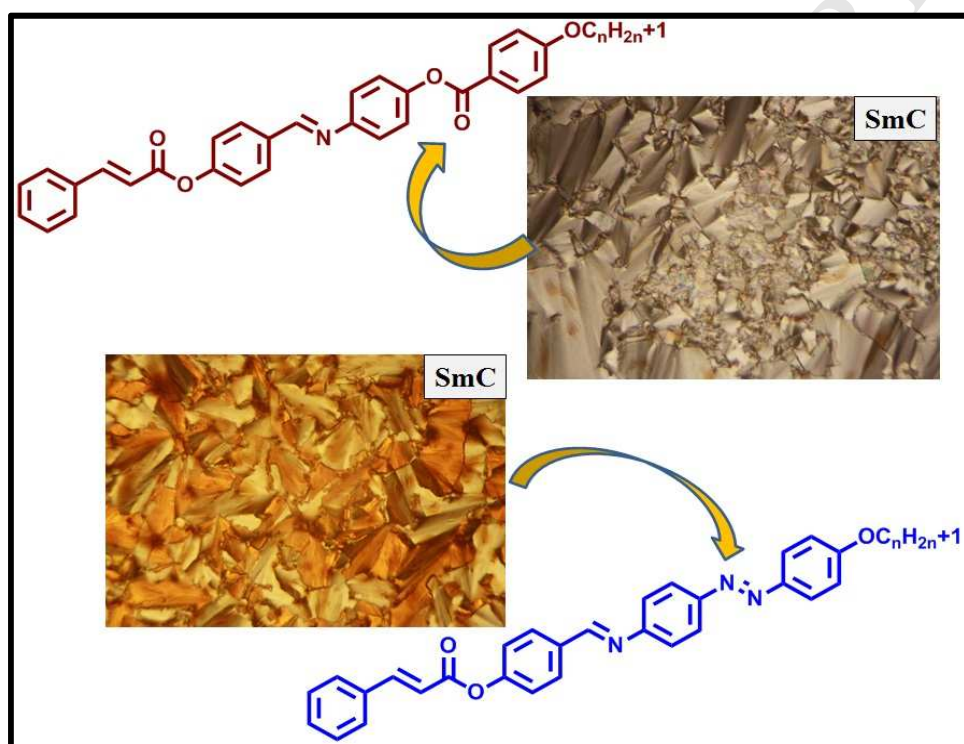
This is a PDF file of an unedited manuscript that has been accepted for publication. As a service to our customers we are providing this early version of the manuscript. The manuscript will undergo copyediting, typesetting, and review of the resulting proof before it is published in its final form. Please note that during the production process errors may be discovered which could affect the content, and all legal disclaimers that apply to the journal pertain.

**Effect of azo and ester linkages on rod shaped Schiff base liquid crystals and their
Photophysical investigations**

Chinnaiyan Selvarasu and Palaninathan Kannan*

Department of Chemistry, Anna University, Chennai, 600 025, India.

Graphical Abstract



**Effect of azo and ester linkages on rod shaped Schiff base liquid crystals and their
Photophysical investigations**

Chinnaiyan Selvarasu and Palaninathan Kannan*

Department of Chemistry, Anna University, Chennai, 600 025, India.

Abstract

Two new series of rod shaped Schiff base containing liquid crystal compounds with azo and ester linkages have been synthesized and characterized respectively. The rod like molecules containing cinnamate linkages with four different alkyl spacers ($n = 6, 8, 10$ and 12) and influence of linking group have been elucidated. Considerable changes in mesomorphic properties were noticed starting from Nematic to Smectic-C on changing of azo and ester linkages along with different terminal alkyl chain lengths. The mesomorphic properties of both series are compared. Photosensitive azobenzene group undergoes photoisomerization under UV light and monitored by UV-Visible spectroscopy.

Keywords: Cinnamate ester, calamitic liquid crystal, azobenzene, photoisomerization, Schiff base

*Corresponding author. Tel: +91 44 22358666, fax: +91 44 2220 0660.

E-mail address: pakannan@annauniv.edu (P. Kannan).

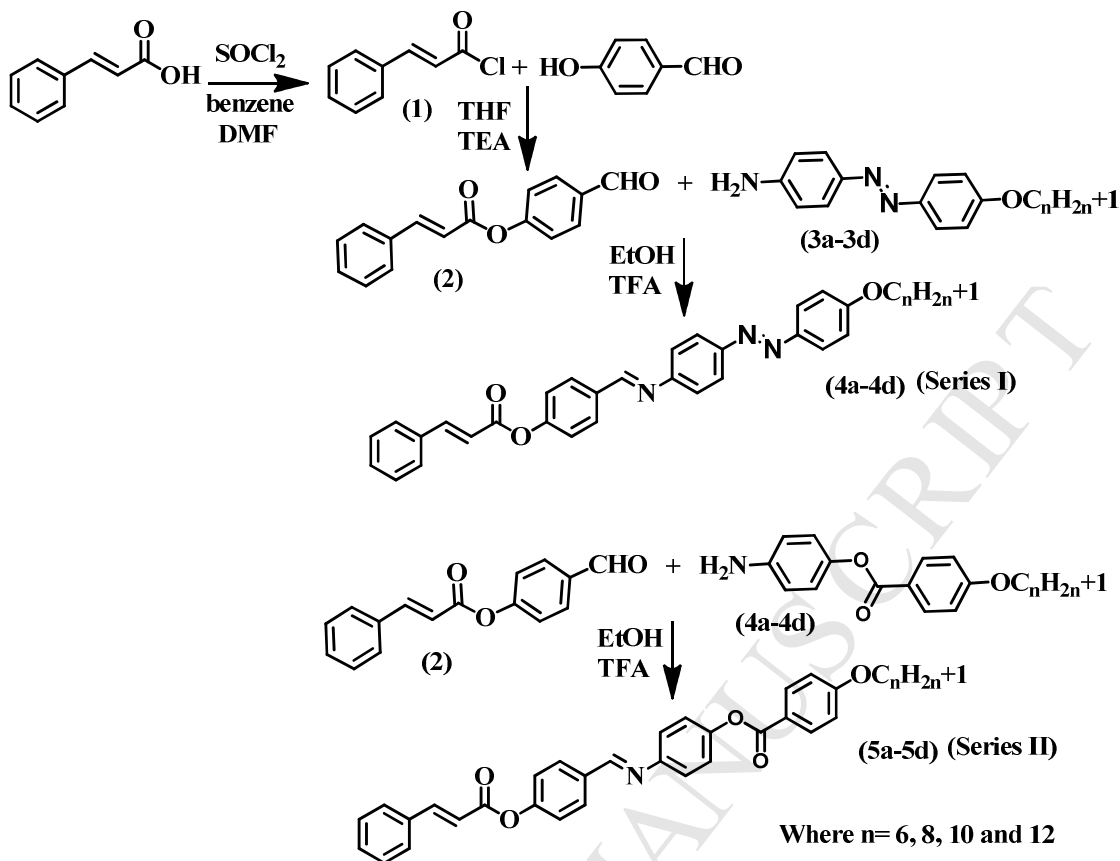
1. Introduction

Azobenzene based liquid crystalline material have been frequently discussed for their sensitivity of chromophoric group towards light and found to exhibit interesting optical properties, enable us to study the materials in holography, optical storage device, optical switching and establish widespread applications in display technology [1–5]. By virtue of their fluidity and translational periodicity, liquid crystal molecules are more easily induced into a new arrangement when triggered by an electric field, [6,7] temperature, [8–10] and light [11–16]. Photo-induced phenomenon is one of the research domain which include incident light brings about molecular ordering and disordering of liquid crystalline system [17]. The designing of liquid crystalline compounds containing double bond as an additional functional group in their molecular structure brings special features. The double bond present in cinnamic acid has already been of research interest in the domain of liquid crystals [18]. Thus upon bringing a double bond in the skeletal frame work enables the compound to have mesomorphic properties, [19] photoisomerization and photocrosslinking in the liquid crystalline state [20].

The rigid skeleton of rod like azobenzene structure and ester linkage aligns themselves as suitable candidates for exhibiting liquid crystal properties [21–24]. Nevertheless, the inimitable characteristics of azobenzene molecules provide prospect of molecular motion in response to heat or light and thus offer many chances in photonic applications. The azo moiety is usually incorporated into cinnamate ester backbone to form liquid crystal depending upon the terminal substituents of azobenzenes [25]. Azobenzene molecules are known to exhibit reversible photoisomerization transformations upon irradiation with UV-visible light [26]. Azo linkage based low and high molecular weight liquid crystalline materials have received attention ascribed to their unique photo-switchable properties induced by light [27–30]. This reveals that azo-cinnamate ester with Schiff base linkage in the skeleton of compound have advantages over substances with other linkages such as ester and silyl group. Several studies reported on ester with Schiff base containing benzene and naphthalene core on liquid crystals. Dave and Prajapati [31] have synthesized rod like liquid crystal materials for number of Schiff base homologous series containing naphthalene moiety. Recently, Prajapati et al have also reported a few mesogenic homologous series of Schiff base esters [32] and azo-esters [33] based rod like mesomorphic nature of naphthalene group.

In the present work, an attempt has been made to study the mesophase stabilities of azomethine-azo and azomethine-ester as part of the frame work which hitherto unreported in the literature. This led us to prepare such compounds that would help further in understanding the effect of central linkage and spacer length on mesomorphism. Herein, the Schiff base containing two series of molecules consist of linking group azo and ester respectively connected to terminal alkyl chains with even number of carbon atoms (6, 8, 10 and 12). Furthermore, this observation assumes significance from the fact that introduction of azo linkage in the first series involve in a new dimension to this field, namely photochromism. These cinnamate ester based azobenzene groups undergo photochemical process in tetrahydrofuran also discussed. The two series have rod shaped cinnamate molecules bearing one side alkyl chain length with azomethine-azo and ester- azomethine linkages respectively with different chain length. Being geometrically closely related to known rod shaped molecules, upon introduction of cinnamate group, containing azo and ester linkages, these systems provided improved liquid crystalline property.

The mesomorphic behaviour was controlled mainly by length of alkyl chain and olefinic character containing cinnamate group. The amine containing azo and ester linking group connected to central core of cinnamate linkage to form Schiff base and changes mesomorphic textures with unique sequence of Nematic and Smectic phases have been noticed. Structural parameters of different calamitic phases were analysed and compared. The synthesis of rod shaped liquid crystal compounds is depicted in Scheme 1.



Scheme 1: Synthesis of rod shaped liquid crystal compounds.

2. Experimental

2.1 Techniques and Materials

All the chemicals and solvents were obtained from commercial sources. The crude samples were purified by column chromatography using silica gel (400 mesh). Thin layer chromatography was performed on aluminium sheets pre-coated with silica gel (Merck, Kieselge 60 and F254). The infrared spectra of compounds were recorded using KBr disk in Perkin Elmer FT-IR spectrometer. ^1H (400 MHz) and ^{13}C NMR (100 MHz) spectra were performed on a Bruker spectrometer using TMS as an internal standard. Compositions of the compounds were determined by Heraeus CHN elemental analyzer. The enthalpies of transitions were determined from thermogram recorded on a differential scanning calorimeter on heating/cooling run at a rate of $5\text{ }^\circ\text{C min}^{-1}$. The transition temperatures for the compounds were determined using a Linkem HFS91 hot stage and controlled processor in conjunction with Linkem HFS91 polarizing optical microscope with a TP-93 temperature programmer connected to 1000D camera. Samples were placed in between two thin glass cover slips and melted with heating and cooling at the rate of $2\text{ }^\circ\text{C min}^{-1}$. UV absorption spectra were

recorded on a UV-1650PC UV-Vis absorption spectrophotometer (Shimadzu). The chloroform solution was prepared with concentration of 1×10^{-5} M.

2.2 Synthesis of 4-formylphenyl cinnamate (2)

The cinnamoyl acid chloride (**1**) (5 gm, 3.37 mmol) was added drop wise to the reaction mixture containing 4-hydroxybenzaldehyde (4.12 gm, 3.37 mmol) and triethylamine (3.35 mmol) dissolved in dry THF and stirred for 24 h. After completion of reaction, triethylamine hydrochloride was precipitated out and removed by filtration. The crude product was subjected to column chromatography (hexane:ethylacetate (95:5%)) to obtain colorless compound **2**. Yield: 77%. M.p: 120 °C. Anal. Calcd for $C_{16}H_{12}O_3$: C, 76.18; H, 4.79. Found (%): C 75.72, H 4.21. FT-IR (KBr pellet, cm^{-1}): 2856–2921 cm^{-1} (C–H str. aliphatic), 1727 cm^{-1} (C=O str. of ester), 1608 cm^{-1} (–C=C– str. vinyl group of cinnamate), 1494 cm^{-1} (C=C str. of aromatic), 1255 – 1023 cm^{-1} (C–O–C str. of alkoxy), 1102 cm^{-1} (C–O str. of ester). 1H NMR (400 MHz, $CDCl_3$) δ 9.90 (s, 1H, CHO), 7.86(d, 2H J = 8.6 Hz, aromatic-H), 7.84 (d, 2H, J = 8.6 Hz, aromatic-H), 7.83 (d, 2H, J = 8.3 Hz, aromatic-H), 7.79 (d, 2H, J = 8.5 Hz, aromatic-H), 7.31- 7.28 (d, 1H, J = 8.1 Hz, aromatic-H), 7.51 (d, J = 14.2 Hz, 1H, olefinic-H), 6.56- 6.52 (d, J = 14.4 Hz, 1H, olefinic- H). ^{13}C NMR (100 MHz, $CDCl_3$) δ 115.54, 121.38, 127.39, 128.03, 130.19, 132.88, 146.51, 154.54, 163.59, 189.92.

2.3 Synthesis of 4-(((E)-4-(cinnamoyloxy)benzylidene)amino)phenyl 4-(hexyloxy)benzoate (4a)

4-Aminophenyl 4-(hexyloxy)benzoate (**3**)(0.1 gm, 0.39 mmol) and 4-formylphenyl cinnamate (**2**, 0.15 gm, 117 mmol) were mixed with ethanol (20 ml), one drop of TFA was added and refluxed for 24 h. The solid obtained after evaporation of chloroform was recrystallized from ethanol. The similar procedure was adapted to synthesis other alkyl compounds (**4b**, **4c** and **4d**; Scheme 1) with yield: 57 %. Anal. Calcd for $C_{34}H_{33}N_3O_3$: C, 76.81; N, 7.90; H, 6.26. Found (%): C, 75.72; N, 7.07; H, 5.69. FT-IR (KBr pellet, cm^{-1}): 2852–2914 cm^{-1} (C–H str. aliphatic), 1732 cm^{-1} (C=O str. of ester), 1605 cm^{-1} (–C=C– str. vinyl group of cinnamate), 1472 cm^{-1} (N=N), 1496 cm^{-1} (C=C str. of aromatic), 1254 – 1027 cm^{-1} (C–O–C str. of alkoxy), 1103 cm^{-1} (C–O str. of ester). 1H NMR (400 MHz, $CDCl_3$): δ 8.48 (s, Ar-CH=N-, 1H), 7.92 – 7.89 (d, J = 7.7 Hz, Aromatic-H, 2H), 7.94 (d, J = 7.8 Hz, Aromatic-H, 6H), 7.51 - 7.35 (m, 5H, aromatic-H), 7.19 (d, J = 7.7 Hz, Aromatic-H, 2H), 7.15 -7.17 (d, J = 7.9 Hz, Aromatic-H, 2H), 7.48 (d, J = 12.7 Hz, olefinic-H, 1H), 6.61 (d, J = 11.6 Hz, olefinic-H, 1H), 4.07 – 3.95 (t, 2H, J = 8.1 Hz, -OCH₂), 1.86 – 1.74 (d, 2H, aliphatic-

CH₂), 1.31 – 1.06 (m, aliphatic-CH₂, 8H), 0.91 – 0.86 (t, 3H, J = 6.6 Hz, aliphatic-CH₃). ¹³C NMR (100 MHz, CDCl₃): 14.3, 22.5, 26.6, 28.6, 29.2, 31.7, 69.7, 115.3, 121.7, 123.5, 124.4, 128.4, 129.3, 131.6, 144.4, 147.6, 151.4, 155.7, 162.5, 163.2, 168.4.

4b: Yield: 61 %. Anal. Calcd for C₃₆H₃₇N₃O₃: C, 77.25; N, 6.66; H, 7.51. Found (%): C, 76.83; N, 6.11; H, 6.82. FT-IR (KBr pellet, cm⁻¹): 2849–2914 cm⁻¹ (C–H str. aliphatic), 1729 cm⁻¹ (C=O str. of ester), 1607 cm⁻¹ (–C=C– str. vinyl group of cinnamate), 1478 cm⁻¹ (N=N), 1502 cm⁻¹ (C=C str. of aromatic), 1252 – 1025 cm⁻¹ (C–O–C str. of alkoxy), 1108 cm⁻¹ (C–O str. of ester). ¹H NMR (400 MHz, CDCl₃): δ 8.48 (s, Ar-CH=N-, 1H), 7.93 – 7.94 (d, J = 7.5 Hz, Aromatic-H, 2H), 7.93 (d, J = 7.7 Hz, Aromatic-H, 6H), 7.58 – 7.25 (m, 5H, aromatic-H), 7.15 (d, J = 7.6 Hz, Aromatic-H, 2H), 7.21 – 7.19 (d, J = 7.29 Hz, Aromatic-H, 2H), 7.48 (d, J = 12.3 Hz, olefinic-H, 1H), 6.52 (d, J = 11.9 Hz, olefinic-H, 1H), 4.05 – 3.96 (t, 2H, J = 8.3 Hz, -OCH₂), 1.89 – 1.72 (d, 2H, aliphatic-CH₂), 1.37 – 1.03 (m, aliphatic-CH₂, 12H), 0.96 – 0.94 (t, 3H, J = 6.8 Hz, aliphatic-CH₃). ¹³C NMR (100 MHz, CDCl₃): 14.2, 22.5, 26.6, 28.4, 29.2, 31.5, 69.7, 115.3, 121.6, 123.4, 124.7, 128.3, 129.8, 131.4, 144.8, 147.4, 151.2, 155.3, 162.7, 163.3, 168.2.

4c: Yield: 63 %. Anal. Calcd for C₃₈H₄₁N₃O₃: C, 77.65; N, 7.15; H, 7.03. Found (%): C, 77.15; N, 7.01; H, 6.81. FT-IR (KBr pellet, cm⁻¹): 2847–2919 cm⁻¹ (C–H str. aliphatic), 1739 cm⁻¹ (C=O str. of ester), 1603 cm⁻¹ (–C=C– str. vinyl group of cinnamate), 1477 cm⁻¹ (N=N), 1498 cm⁻¹ (C=C str. of aromatic), 1254 – 1025 cm⁻¹ (C–O–C str. of alkoxy), 1108 cm⁻¹ (C–O str. of ester). ¹H NMR (400 MHz, CDCl₃): δ 8.52 (s, Ar-CH=N-, 1H), 7.92 – 7.90 (d, J = 7.5 Hz, Aromatic-H, 2H), 7.93 (d, J = 7.3 Hz, Aromatic-H, 6H), 7.42 – 7.31 (m, 5H, aromatic-H), 7.16 (d, J = 7.5 Hz, Aromatic-H, 2H), 7.15 – 7.17 (d, J = 7.5 Hz, Aromatic-H, 2H), 7.48 (d, J = 12.2 Hz, olefinic-H, 1H), 6.49 (d, J = 11.8 Hz, olefinic-H, 1H), 4.06 – 3.97 (t, 2H, J = 8.4 Hz, -OCH₂), 1.86 – 1.79 (d, 2H, aliphatic-CH₂), 1.35 – 1.09 (m, aliphatic-CH₂, 16H), 0.98 – 0.96 (t, 3H, J = 6.8 Hz, aliphatic-CH₃). ¹³C NMR (100 MHz, CDCl₃): 14.1, 22.8, 26.6, 28.6, 29.2, 31.5, 69.4, 115.6, 121.4, 123.4, 124.6, 128.3, 129.2, 131.5, 144.5, 147.3, 151.6, 155.4, 162.6, 163.2, 168.2.

4d: Yield: 61 %. Anal. Calcd for C₄₀H₄₅N₃O₃: C, 78.02; N, 6.82; H, 7.37. Found (%): C, 77.85; N, 5.62; H, 7.12. FT-IR (KBr pellet, cm⁻¹): 2848–2915 cm⁻¹ (C–H str. aliphatic), 1735 cm⁻¹ (C=O str. of ester), 1601 cm⁻¹ (–C=C– str. vinyl group of cinnamate), 1473 cm⁻¹ (N=N), 1499 cm⁻¹ (C=C str. of aromatic), 1250 – 1022 cm⁻¹ (C–O–C str. of alkoxy), 1106 cm⁻¹ (C–O str. of ester). ¹H NMR (400 MHz, CDCl₃): δ 8.51 (s, Ar-CH=N-, 1H), 7.94 – 7.92

(d, $J = 7.8$ Hz, Aromatic-H, 2H), 7.91 (d, $J = 7.54$ Hz, Aromatic-H, 6H), 7.44 - 7.33 (m, 5H, aromatic-H), 7.17 (d, $J = 7.43$ Hz, Aromatic-H, 2H), 7.13 - 7.11(d, $J = 7.43$ Hz, Aromatic-H, 2H), 7.50 (d, $J = 12.5$ Hz, olefinic-H, 1H), 6.60 (d, $J = 11.7$ Hz, olefinic-H, 1H), 4.02 - 3.99 (t, 2H, $J = 8.2$ Hz, -OCH₂), 1.81 - 1.75 (d, 2H, aliphatic-CH₂), 1.32 - 1.00 (m, aliphatic-CH₂, 20H), 0.99 - 0.97 (t, 3H, $J = 6.4$ Hz, aliphatic-CH₃). ¹³C NMR (100 MHz, CDCl₃): 14.0, 22.9, 26.4, 28.7, 29.0, 31.6, 69.6, 115.5, 121.7, 123.3, 124.5, 128.6, 129.1, 131.3, 144.7, 147.7, 151.5, 155.1, 162.4, 163.0, 168.0.

2.4 Synthesis of 4-((E)-(4-(cinnamoyloxy)benzylidene)amino)phenyl 4-(hexyloxy)benzoate (5a):

A similar synthetic procedure (**4a**) was employed in the second series for the preparation of 4-((E)-(4-(cinnamoyloxy)benzylidene)amino)phenyl 4-(hexyloxy)benzoate (**5a**) by changing the reactant to 4-aminophenyl 4-(hexyloxy)benzoate (**3a**). The similar procedure was adapted to synthesis other alkyl compounds (**5b**, **5c** and **5d**; Scheme 1) with yield: 57 %. Anal. Calcd for C₃₅H₃₃NO₅: C, 76.76; N, 2.56; H, 6.07 %; Found (%): C, 76.22; N, 2.02; H, 5.58. FT-IR (KBr pellet, cm⁻¹): 2847-2922 cm⁻¹ (C-H str. aliphatic), 1729 cm⁻¹ (C=O str. of ester), 1606 cm⁻¹ (-C=C- str. vinyl group of cinnamate), 1494 cm⁻¹ (C=C str. of aromatic), 1254 - 1028 cm⁻¹ (C-O-C str. of alkoxy), 1106 cm⁻¹ (C-O str. of ester). ¹H NMR (400 MHz, CDCl₃): δ 8.70 (s, Ar-CH=N-, 1H), 8.12 - 8.04 (d, $J = 7.6$ Hz, Aromatic-H, 2H), 7.52 (d, $J = 7.5$ Hz, Aromatic-H, 6H), 7.37 - 7.32 (m, 5H, aromatic-H), 7.15 (d, $J = 7.5$ Hz, Aromatic-H, 2H), 7.18 - 7.08 (d, $J = 7.6$ Hz, Aromatic-H, 2H), 7.43 (d, $J = 11.7$ Hz, olefinic-H, 1H), 6.74 - 6.71 (d, $J = 11.5$ Hz, olefinic-H, 1H) 4.02 - 3.98 (t, 2H, $J = 8.2$ Hz, OCH₂), 1.74 - 1.72 (d, 2H, aliphatic-CH₂), 1.52 - 1.21 (m, 6H, aliphatic-CH₂), 1.02 - 0.98 (t, 3H, $J = 6.7$ Hz, aliphatic-CH₃). ¹³C NMR (100 MHz, CDCl₃): 14.1, 22.8, 26.5, 28.6, 29.1, 31.5, 69.6, 114.6, 115.3, 119.2, 121.7, 122.7, 123.6, 128.6, 129.0, 131.2, 132.3, 134.5, 135.8, 144.6, 146.4, 150.4, 155.2, 163.9, 167.1, 168.1.

5b: Yield: 62 %. Anal. Calcd for C₃₇H₃₇NO₅: C, 77.19; N, 2.43; H, 6.48 %. Found (%): C, 76.82; N, 2.16; H, 6.12. FT-IR (KBr pellet, cm⁻¹): 2856-2925 cm⁻¹ (C-H str. aliphatic), 1731 cm⁻¹ (C=O str. of ester), 1606 cm⁻¹ (-C=C- str. vinyl group of cinnamate), 1499 cm⁻¹ (C=C str. of aromatic), 1254 - 1026 cm⁻¹ (C-O-C str. of alkoxy), 1102 cm⁻¹ (C-O str. of ester). ¹H NMR (400 MHz, CDCl₃): δ 8.68 (s, Ar-CH=N-, 1H), 8.12 - 8.08 (d, $J = 7.6$ Hz, Aromatic-H, 2H), 7.7 (d, $J = 7.4$ Hz, Aromatic-H, 6H), 7.36 - 7.31 (m, 5H, aromatic-H), 7.16 (d, $J = 7.6$ Hz, Aromatic-H, 2H), 7.19 - 7.14 (d, $J = 7.4$ Hz, Aromatic-H, 2H), 7.47 (d, $J = 11.7$ Hz, olefinic-H, 1H), 6.72 - 6.70 (d, $J = 11.4$ Hz, olefinic-H, 1H), 4.02 - 3.98 (t, 2H, $J = 8.4$ Hz, OCH₂), 1.76 - 1.72 (d, 2H, aliphatic-CH₂), 1.50 - 1.24 (m, 10H, aliphatic-CH₂), 1.02 - 0.98

(t, 3H, $J = 6.7$ Hz, aliphatic-CH₃). ¹³C NMR (100 MHz, CDCl₃): 14.2, 22.7, 26.6, 28.5, 29.2, 31.4, 69.5, 114.6, 115.3, 119.2, 121.7, 122.7, 123.4, 128.5, 129.1, 131.3, 132.2, 134.5, 135.6, 144.6, 146.5, 150.4, 155.2, 163.8, 167.2, 168.1.

5c: Yield: 57 %. Anal. Calcd for C₃₉H₄₁NO₅: C, 77.59; N, 2.32; H, 6.84 %. Found (%): C, 77.25; N, 1.67; H, 6.22. FT-IR (KBr pellet, cm⁻¹): 2854–2928 cm⁻¹ (C–H str. aliphatic), 1725 cm⁻¹ (C=O str. of ester), 1608 cm⁻¹ (–C=C– str. vinyl group of cinnamate), 1494 cm⁻¹ (C=C str. of aromatic), 1262–1016 cm⁻¹ (C–O–C str. of alkoxy), 1108 cm⁻¹ (C–O str. of ester). ¹H NMR (400 MHz, CDCl₃): δ 8.69 (s, Ar-CH=N-, 1H), 8.12–8.05 (d, $J = 7.4$ Hz, Aromatic-H, 2H), 7.51 (d, $J = 7.5$ Hz, Aromatic-H, 6H), 7.37–7.34 (m, 5H, aromatic-H), 7.16 (d, $J = 7.6$ Hz, Aromatic-H, 2H), 7.19–7.12 (d, $J = 7.6$ Hz, Aromatic-H, 2H), 7.51 (d, $J = 11.4$ Hz, olefinic-H, 1H), 6.71–6.68 (d, $J = 11.4$ Hz, olefinic-H, 1H) 4.02–3.98 (t, 2H, $J = 8.4$ Hz, OCH₂), 1.74–1.70 (d, 2H, aliphatic-CH₂), 1.51–1.21 (m, 14H, aliphatic-CH₂), 1.0–0.98 (t, 3H, $J = 6.5$ Hz, aliphatic-CH₃). ¹³C NMR (100 MHz, CDCl₃): 14.1, 22.6, 26.5, 28.6, 29.1, 31.5, 69.6, 114.5, 115.4, 119.2, 121.5, 122.8, 123.4, 128.4, 129.1, 131.4, 132.3, 134.2, 135.6, 144.6, 146.4, 150.3, 155.2, 163.7, 167.2, 168.1.

5d: Yield: 54 %. Anal. Calcd for C₄₁H₄₅NO₅: C, 77.94; N, 2.22; H, 7.18 %. Found (%): C, 77.23; N, 1.87; H, 7.02. FT-IR (KBr pellet, cm⁻¹): 2853–2929 cm⁻¹ (C–H str. aliphatic), 1729 cm⁻¹ (C=O str. of ester), 1608 cm⁻¹ (–C=C– str. vinyl group of cinnamate), 1502 cm⁻¹ (C=C str. of aromatic), 1258–1029 cm⁻¹ (C–O–C str. of alkoxy), 1107 cm⁻¹ (C–O str. of ester). ¹H NMR (400 MHz, CDCl₃): δ 8.71 (s, Ar-CH=N-, 1H), 8.11–8.09 (d, $J = 7.5$ Hz, Aromatic-H, 2H), 7.54 (d, $J = 7.6$ Hz, Aromatic-H, 6H), 7.35–7.35 (m, 5H, aromatic-H), 7.17 (d, $J = 7.74$ Hz, Aromatic-H, 2H), 7.16–7.06 (d, $J = 7.52$ Hz, Aromatic-H, 2H), 7.42 (d, $J = 11.6$ Hz, olefinic-H, 1H), 6.75–6.71 (d, $J = 11.6$ Hz, olefinic-H, 1H) 4.01–3.99 (t, 2H, $J = 8.3$ Hz, OCH₂), 1.76–1.71 (d, 2H, aliphatic-CH₂), 1.51–1.23 (m, 18H, aliphatic-CH₂), 1.01–0.99 (t, 3H, $J = 6.4$ Hz, aliphatic-CH₃). ¹³C NMR (100 MHz, CDCl₃): 14.0, 22.9, 26.4, 28.7, 29.0, 31.6, 69.6, 114.7, 115.3, 119.1, 121.7, 122.9, 123.6, 128.6, 129.0, 131.1, 132.3, 134.5, 135.8, 144.7, 146.4, 150.5, 155.1, 163.9, 167.1, 168.0.

3. Results and discussion

3.1 Molecular structural characterization

4-(((E)-4-(cinnamoyloxy)benzylidene)amino)phenyl 4-(alkyloxy)benzoate (series **I**) and 4-((E)-4-(cinnamoyloxy)benzylidene)amino)phenyl 4-(alkylxoy)benzoate (series **II**)

comprising azo-Schiff base and ester-Schiff base as a central linkage respectively were synthesized to investigate the influence of functional groups on Schiff base. In both series, alkoxy chain is attached in one side in the terminal position. Their chemical structures are confirmed by spectroscopic studies. $^1\text{H-NMR}$ spectrum of compound **2** revealed that aldehyde proton signal at 9.98 ppm and imine proton in the Schiff base (**4d**) in signal in the range of 8.38–8.45 ppm were observed. ^{13}C NMR spectrum of compound **2**, the aldehyde exhibits a resonance signal at 189.92 ppm and in the Schiff base **4d**; the imine exhibits a resonance signal at 163.96 ppm. The presence of intermediate compound having aldehyde and imine group of Schiff base compound in the similar structure of **5d** were confirmed by Fourier transform infrared (FT-IR) spectroscopy, since in each case the band characteristic of $-\text{CH}=\text{N}-$ stretching deformations was detected. The exact position of this band varies in the spectral range of $1601\text{--}1620\text{ cm}^{-1}$ (see experimental details). In accordance with NMR and FT-IR data collected in the experimental section, spectral data obtained are in agreement with data predicted from chemical formulae of synthesized compounds. Purity of all imines compounds was confirmed by elemental analysis. Elemental analysis indicated quite good agreement with calculated values of carbon, nitrogen and hydrogen in the compounds.

3.2 Mesomorphic properties

The mesomorphic properties of all the synthesized compounds have been characterized by differential scanning calorimetry and polarizing optical microscopy attached with a hot stage. Thin-film samples were obtained by sandwiching them between a glass slides with cover slip. All the compounds of **I** and **II** series exhibited mesomorphism. On cooling, isotropic liquids of **I** and **II** series compounds with $n=6$ formed small droplets that coalesced to classical schlieren texture of Nematic phase while, $n=8$ and 10 derivatives exhibited focal-conic texture, characteristic of Nematic phases. On increasing chain length ($n=12$), they display Nematic and focal conic texture characteristic of Smectic-C mesophase when cooled from isotropic liquid. The Nematic mesophase prevails ascribed to terminal alkoxy chain attractions are more pronounced. The lower homologous members exhibit purely Nematic mesophase. The **I** and **II** series have cinnamoyloxy connected with azo and ester central linkage in addition to double bond that increases length and polarizability. The presence of double bond leads to form rod like molecules and enhances mesophase thermal stability. Therefore the greater mesophase thermal stability of the present **I** and **II** series can be explained in terms of greater molecular length and polarizability of molecule resulting from additional $-\text{CH}=\text{CH}-$ units in the central linkage.

It is inferred that as the series is ascended, the overall polarizability is enhanced with increase in alkyl chain length [34]. The ratio of terminal attractions to lateral attractions decreases as the series is descended; the net result is that the lateral attractions gain prevalence over the terminal attractions. The molecules under such conditions will observe, strictly maintaining the layered structure, although they might partially attain a fluid condition. Under such situations, the layered Smectic texture is maintained, giving rise to a Smectic mesophase. As the temperature is further increased, the strict performance of molecules in the layered form is weakened ascribed to increased thermal vibrations. The molecules slowly acquire a more fluid nature, although they do not abruptly attain any randomness. At a definite temperature, the layered structure breaks down, but end-to-end parallel orientation is still maintained, giving rise to more fluidity and a Nematic threaded texture to the molecules. Smectic-C mesophase is exhibited from decyloxy derivative onwards. The overall polarizability of the molecules is enhanced as the alkyl chain length at one end increases, contributing to the exhibition of Smectic texture [35]. However, ratio of terminal to lateral attractions is also low at a certain stage, leading to thermal vibration break down the orientation of molecules without giving them a chance for adopting Nematic orientation. Thus, only a Smectic-C mesophase prevails in dodecyloxy derivative. DSC is a valuable tool for detection of phase transition temperature. It yields quantitative results; therefore conclusions may be drawn concerning the nature of phases which participate in the transition. The **4a-4d** and **5a-5d** compounds consist of aromatic ring depend upon the **I - II** series including cinnamate as central core for the rod shaped molecule.

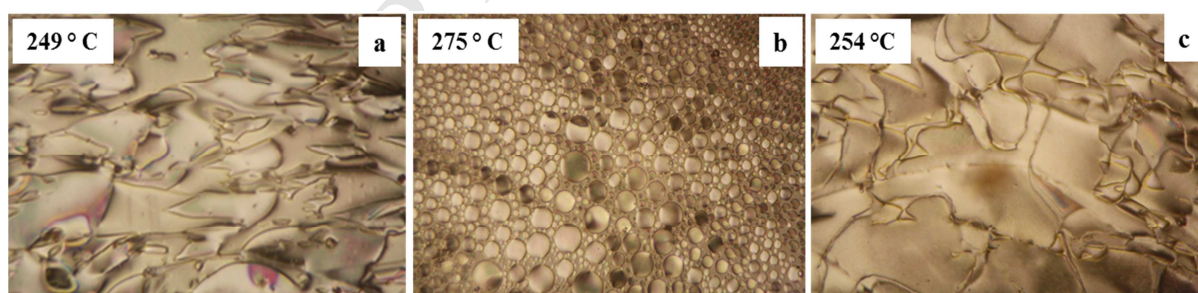


Figure 1. Microphotographs texture observed for different phases for compound **4a**. **a)** Schlieren texture of Nematic phase at 249 °C for heating (**b** & **c**) Nematic droplet and Nematic phase on cooling at 275 °C and 254 °C.

The DSC data of **4d**, **5d** were recorded in the first heating cycle as a representative example for each series and investigated in detail. The phase transition temperatures and corresponding enthalpy changes of compounds were determined using DSC. The data

obtained from DSC analysis are summarized in Table 1, which helps us to further confirm mesophase type. The calamitic liquid crystal textures of compounds were observed on polarized optical microscope in the range of 35 – 295 °C upon heating and cooling cycle at 20X magnification.

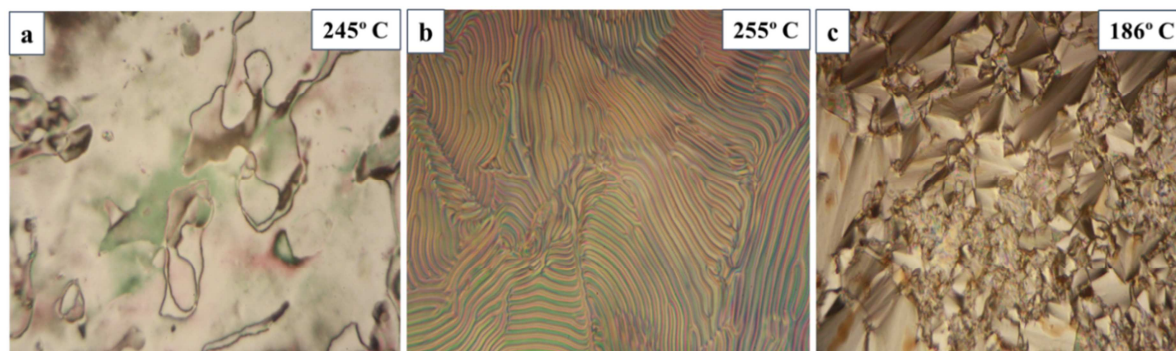


Figure 2. Microphotographs of texture observed for compound **4d**. (a) Schlieren texture of Nematic phase on heating at 245 °C. (b & c) Cholesteric fingerprint region and Sm-C phases at 255 and 186 °C upon cooling.

The peak temperatures were consistent with those inferred from optical experiments. Normally, calamitic liquid crystals of lower alkyl chain are Nematic, the medium length of alkyl chain exhibit Nematic and Smectic phases; on the other hand, higher members are entirely Smectic-C in nature [36]. Upon heating and cooling **4a** exhibits two transitions, in which transitions from crystal to Nematic and Nematic to isotropic occurs while heating to 285 °C and reverse transitions occur on cooling to 169 °C, respectively as displayed in Fig.1.

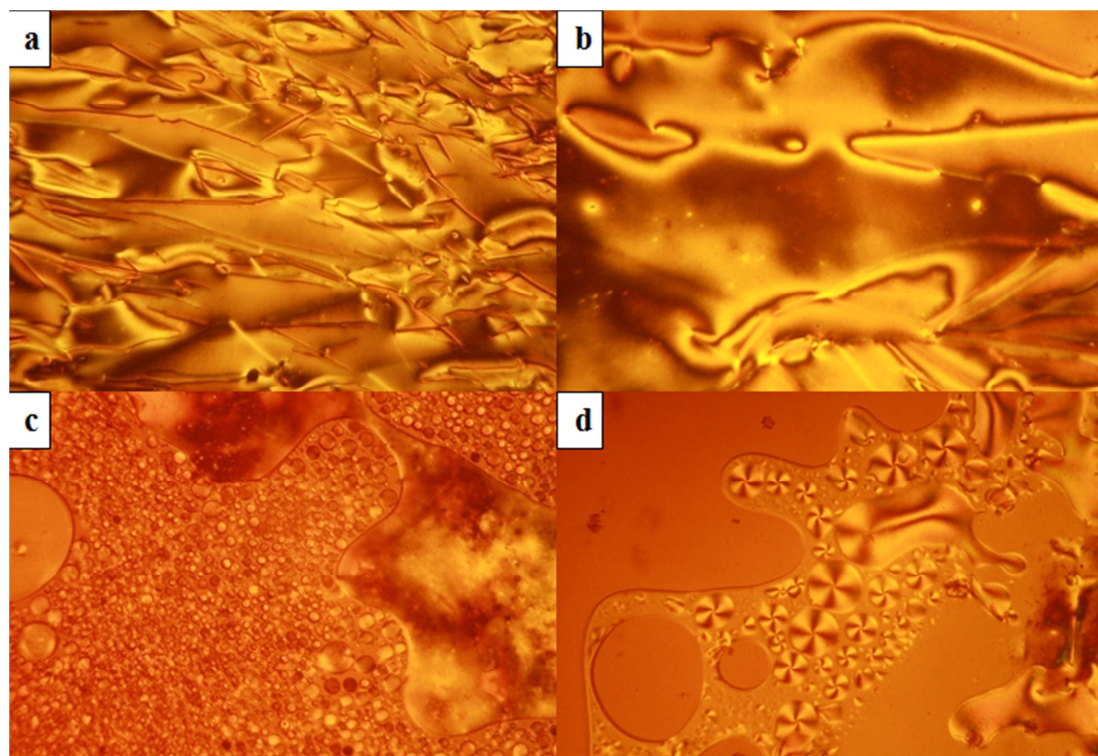


Figure 3. Microphotographs texture observed for liquid crystalline textures for compound **5a**. (a & b) Nematic phase at 249 and 266 °C on heating (c & d) Nematic droplet and Nematic phase on cooling at 271 °C and 260 °C.

The **4d** revealed two phases on heating which corresponds to crystal-Nematic and Nematic–isotropic phase to 275 °C while cooling from isotropic, Nematic droplet was observed and further cooling, Cholesteric finger print region were exhibited at 255 °C and promote cooling a typical fan shaped texture for Smectic-C phase was observed at 186 °C as exhibited in Fig.2.

Table 1. Phase transition temperatures (T/°C) and enthalpies ($\Delta H/J g^{-1}$) obtained from DSC scans of compounds 4a-4d and 5a-5d.

Compound	Heating	Cooling cycle
4a	Cr 143.9 (15.5) N 285.4 (2.21) I	I 281.7 (-0.2) N 169.9 (-21.5) Cr
4b	Cr 140.1 (21.75) N 281.7 (2.13) I	I 277.2 (-0.1) N 162.6 (-25.7) Cr
4c	Cr 137.7 (29.54) N 278.1 (1.62) I	I 273.7 (-0.5) N 152.4 (-29.2) Cr
4d	Cr 135.4 (32.51) N 275.2 (1.36) I	I 270.4 (-0.4) N 266.6 (2.45) SmC 148.7 (-33.5) Cr
5a	Cr 152.1 (19.75) N 296.6 (0.29) I	I 282.5 (-0.1) N 172.6 (-37.4) Cr
5b	Cr 148.3 (21.42) N 289.9 (0.38) I	I 283.3 (-0.6) N 169.2 (-27.5) Cr
5c	Cr 145.8 (26.14) N 279.3 (0.54) I	I 276.2 (-0.4) N 158.5 (19.5)Cr
5d	Cr 139.2 (30.73) N 275.4 (0.73) I	I 270.4 (-0.3) N 249.6 (-19.7) SmC 151.7 (18.3) Cr

Abbreviations: Cr = Crystal, SmA= Smectic A, N = Nematic, Sm-C = Smectic-C, I = Isotropic

The compound **5a** revealed two endo and exo peaks during first heating and cooling. On cooling the phase sequence found as Crystal–Nematic and Nematic–isotropic while reverse phase occur on cooling as evidenced in Fig. 3 (a–d).

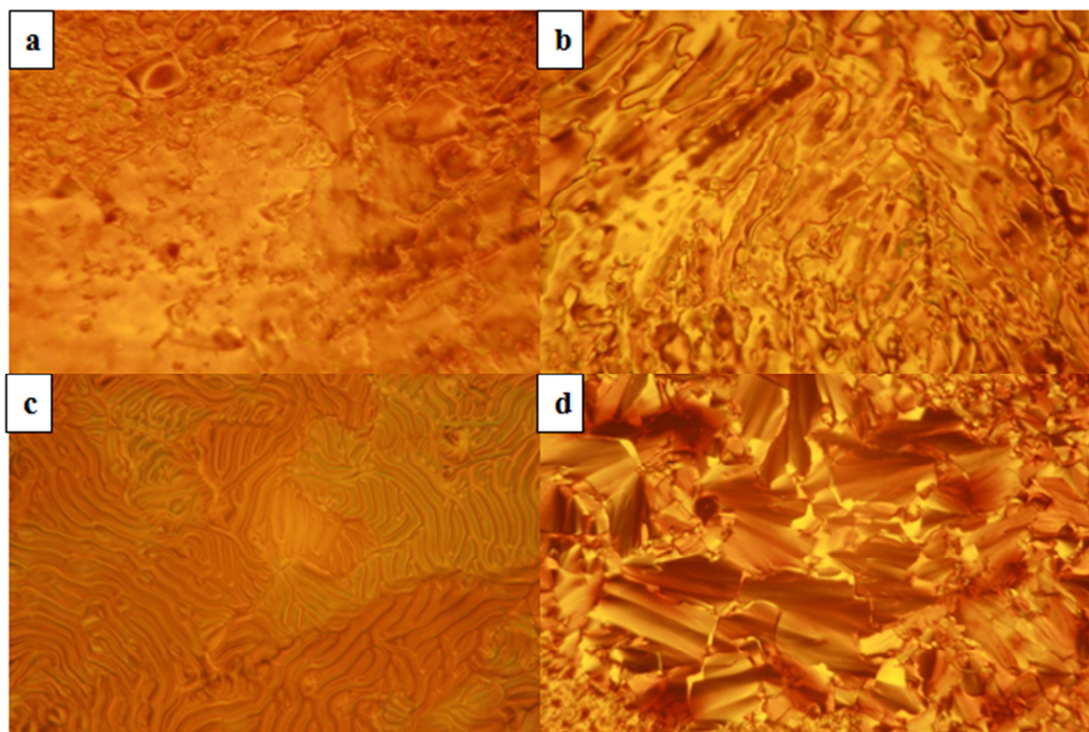


Figure 4. Microphotographs of texture observed for compound **5d**. (a & b) Nematic phases exhibited on heating at 268 °C (b & c) Cholesteric fingerprint region and SmC phases at 256 and 196 °C upon cooling.

The **5d** exhibited Nematic phase for heating at 275 °C as indicated in Fig 4 (a & b). On cooling from isotropic exhibits Nematic to Cholesteric finger print region and Smectic-C phase were observed in Fig.4 (c & d) and crystallized at 122 °C. The remaining lower members of **4b**, **4c** and **5b**, **5c** exhibit from similar observation of Nematic mesophase with wide transition temperature ascribed to flexibility of increased alkyl chain length whereas the phase transition sequence from cooling as Iso–Nematic–Cr. The **5d** exhibit Smectic-C texture because of increased alkyl chain length (n=12) and revealed that crystal mesophase transition temperatures decrease with increase in length of terminal alkyl chain. The Nematic-isotropic transition temperatures also decrease with increase in number of carbon atoms in the alkoxy chain, whereas it exhibits a tendency for rising Smectic-C – Nematic transition temperature in ascending series, which levels off slightly in the higher homologues.

3.3 Photophysical property

Absorption spectra of compound were obtained and their absorption band summarized in Table ST1 and Fig. 5. The absorption spectra of compounds was carried out in tetrahydrofuran solution ($C = 1.1 \times 10^{-3} \text{ mol L}^{-1}$). The compounds were irradiated with UV light (365 nm), the band corresponding to $\pi-\pi^*$ and $n-\pi^*$ transitions decreases with increase in irradiated time. [25] The band corresponding to isomerized product increases by increasing irradiating time and exhibited in Fig.5. The photoisomerization has confirmed and occurred in the range of 380–550 nm.

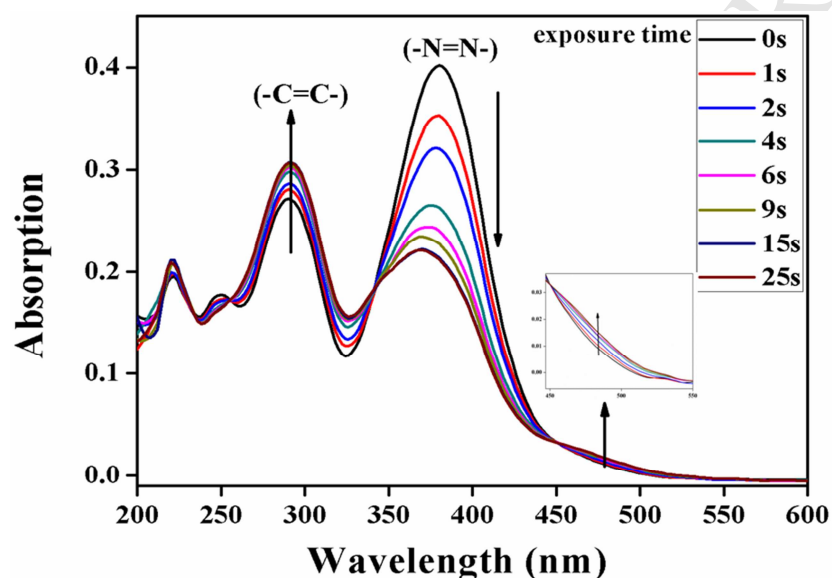


Figure 5. Absorption spectrum of compound **5a**

The **5a** irradiated at 365 nm, E-Z isomerization resulting with a dramatic decrease in absorption band from 382 nm ascribed to $\pi-\pi^*$ transition of trans (E) isomer in azo group. In addition, very weak absorption band is found in the visible region around 505 nm, appropriate to $n-\pi^*$ transition of cis (Z) isomer in azo group which gradually increased by reaching photo stationary state within 25 s. After 25 s illumination, there is no change in absorption spectrum confirms photo saturation of E-Z (trans-cis) isomerization process. The isobestic points were observed at 340 and 470 nm, corresponding to trans-cis isomerization as these suggesting that only two isomers obtained. In Fig.5 another band absorption exhibit compound containing cinnamate unit ($-\text{CH}=\text{CH}-\text{COO}-$) in double bond undergo isomerization around 263 nm. At the same time, we have tried for reversible photo isomerization under dark condition for several minutes in **5a** with same concentration in tetrahydrofuran solution. The transformed cis isomer (Z) is not converted into trans form (E)

due to the imine (-CH=N-) group restricts electron delocalization on cinnamate (-CH=CH-COO-) moiety.

3.4 Comparison of mesophase and thermal property

The azo and ester linkage in the Schiff base at para position in the **I** and **II** series has a pronounced effect on mesophase transition temperatures. Series **I** where the central core is connected to ester linkage demonstrates decrease in stability of the system when compared to azo linkage in series **II**. Moving on further level study, ester linkage consist of ketonic bond where electron density pulled by ester system in the central core that leads to decrease in transition temperatures. On the other hand, in series **II**, the azo linkage in the central core provides rich electron density towards entire system that enhances transition temperature. The mesomorphic properties of entire rod like molecules exhibit good liquid crystalline texture relative on alkyl chain length. The four-aromatic ring containing azo linkage compounds have faster photo isomerization. This may be attributed to the nature of linking group in the azobenzene as well as flexibility of ester moiety. The time taken for photoisomerization depends on nature of linking group and size of substituent in the azobenzene moiety.

4. Conclusion

We have reported the synthesis and characterization of rod shaped liquid crystalline Schiff base containing compounds with azo and ester linkages. The mesophase range of present series **I** is higher than series **II** for those of structurally related compounds possess ester and azo linkage and attributed to high polarizability of the molecules. The effect of terminal alkoxy containing azobenzene moiety, central linkage with or without spacer attached also plays a crucial role in formation of mesophase. The presence of olefinic double bond enhances length of polarizability of rod shaped molecules and increases thermal stability with high polarizability resulting from additional olefinic unit in the linkage. The results provided the understanding of structure–property relationships in liquid crystals. The structural aspects strongly enhance phase transition behaviour of Schiff's base compounds. Very high isotropic transition temperature of >296 °C was observed for azomethine containing cinnamate esters. Interestingly the change in orientation of ester group in lengthening the arm in compounds of series **II** led to decrease of both melting and clearing temperatures. The azobenzene containing ester molecules involves isomerisation. The

duration required for exhibiting the phenomena of photoisomerization mainly depends on nature of the linking group in the azo moiety.

Acknowledgements

C.S and P.K sincerely acknowledge to University Grants Commission, New Delhi, Government of India [39-691/2010 (SR)] for the financial support. Instrumentation facilities provided under DST-FIST, UGC-DRS to Department of Chemistry, Anna University are gratefully acknowledged.

References

- [1] C. Ruslim and K. Ichimura. *J. Mater. Chem.* 9 (1999) 673–681.
- [2] J. Belmar. New liquid crystals containing the benzothiazol unitramides and azo compounds. *Liq. Cryst.* 26 (1999) 396.
- [3] L.L. Lai, E. Wang, Y.H. Liu and Y. Wang. *Liq. Cryst.* 29 (2002) 871–875.
- [4] A.K. Prajapati. *Mol. Cryst. Liq. Cryst.* 364 (2001) 769–777.
- [5] L. Komitov, K. Ichimura, A. Strigazzi. *Liq. Cryst.* 27 (2000) 51–55.
- [6] G.W. Gray. *Thermotropic Liquid Crystals*. Wiley Chichester. 1987.
- [7] E. Smela. *Adv. Mater.* 15 (2003) 481–494.
- [8] C.H. Legge, G.R. Mitchell. *J. Phys. D: Appl. Phys.* 25 (1992) 492–495.
- [9] K. Maeda, H. Mochizuki, M. Watanabe, E. Yashima. *J. Am. Chem. Soc.* 128 (2006) 7639–7650.
- [10] S. Kurihara, T. Ikeda, S. Tazuke. *Mol. Cryst. Liq. Cryst.* 178 (1990) 117–132.
- [11] D. Pijper, M.G.M. Jongejan, A. Meetsma, B.L. Feringa. *J. Am. Chem. Soc.* 130 (2008) 4541–4552.
- [12] D. Pijper, B.L. Feringa. *Soft. Matter.* 4 (2008) 1349–1372.
- [13] Y. Yu, T. Ikeda. *J. Photochem. Photobiol. C* 5 (2004) 247–265.

- [14] T. Ikeda, T. Miyamoto, T. Sasaki, S. Kurihara, S. Tazuke. *Mol. Cryst. Liq. Cryst.* 188 (1990) 235–250.
- [15] T. Ikeda, T. Miyamoto, S. Kurihara, M. Tsukada, S. Tazuke. *Mol. Cryst. Liq. Cryst.* 188 (1990) 207–222.
- [16] M.M. Green, S. Zanella, H. Gu, T. Sato, G. Gottarelli, S.K. Jha, G.P. Spada, A.M. Schoevaars, B. Feringa, A. Teramoto. *J. Am. Chem. Soc.* 120 (1998) 9810–9817.
- [17] (a) S.K. Prasad, G.G. Nair, G. Hegde. *Adv. Mater.* 17 (2005) 2086–2091. (b) D. Tanaka, H. Ishiguro, Y. Shimizu, K. Uchida. *J. Mater. Chem.* 22 (2012) 25065–25071.
- [18] H. Kihara, N. Tamaoki. *Macromol. Rapid. Commun.* 27 (2006) 829–834.
- [19] (a) I.C. Pintre, J.L. Serrano, M. Blanca Ros, J. Martinez-Perdiguero, I. Alonso, J. Ortega, C.L. Folcia, J. Etxebarria, R. Alicante, B. Villacampa. *J. Mater. Chem.* 20 (2010) 2965–2971.
- [20] (a) P.C. Yang, J.H. Liu. *J. Poly. Sci. Part A: Polym. Chem.* 46 (2008) 1289–1304.
- (b) A. Bobrovsky, V. Shibaev, V. Hamplova, M. Kaspar, V. Novotna, M. Glogarova, E. Pozhidaev. *Liq. Cryst.* 36 (2009) 989–997.
- [21] K. Ichimura. *Chem. Rev.* 100 (2000) 1847–1874.
- [22] T. Ikeda. *J. Mater. Chem.* 13 (2003) 2037–2057.
- [23] M. Vijaysrinivasan, P. Kannan, A. Roy. *Liq. Cryst.* 39 (2012) 1465–1475.
- [24] S. Balamurugan, P. Kannan, K. Yadupati, A. Roy. *Liq. Cryst.* 38 (2011) 1199–1207.
- [25] C. Selvarasu, P. Kannan. *J. Mole. Struc.* 1092 (2015) 176–186.
- [26] T. Ikeda, O. Tsutsumi. *Science.* 268 (1995) 1873–1875.
- [27] C. Ruslim, K. Ichimura. *J. Mater. Chem.* 9 (1999) 673–681.
- [28] A. Urbas, V. Tondiglia, L. Natarajan, R. Sutherland, H. Yu, J.H. Li, T. Bunning. *J. Am. Chem. Soc.* 126 (2004) 13580–13581.

- [29] K. Ichimura, S.K. Oh, M. Nakagawa. *Science*. 288 (2000) 1624–1626.
- [30] L. Komitov, C. Ruslim, Y. Matsuzawa, K. Ichimura. *Liq. Cryst.* 27 (2000) 1011–1016.
- [31] J.S. Dave, N.R. Patel, A. Prajapati. *Curr. Sci.* 47 (1978) 425.
- [32] A.K. Prajapati. *Liq. Cryst.* 27 (2000) 1017–1020.
- [33] N.D. Jadav, B.A. Prajapati, A.K. Prajapati. *Mol. Cryst. Liq. Cryst.* 399 (2003) 53–60.
- [34] M. Vijay Srinivasan, P. Kannan, A. Roy. *New. J. Chem.* 37 (2013) 1584–1590.
- [35] N.G. Nagaveni, A. Roy, V. Prasad. *J. Mater. Chem.* 22 (2012) 8948–8959.
- [36] J.M. Lohar, Urvashi Mashru. *Mol. Cryst. Liq. Cryst.* 70 (1981) 29–38.

Research Highlights

- We have synthesized and characterized new rod shaped liquid crystalline compounds.
- Azo and ester linkage affected the mesomorphism.
- All the compounds exhibited good LC mesophase depend upon the alkyl chain length.
- Azo-Schiff base compounds exhibited photoisomerization.